Supporting Information

Valid Design and Evaluation of Cathode and Anode Materials of Aqueous Zinc Ion Batteries with High-Rate Capability and Cycle Stability

Se Hun Lee,[a†] Juyeon Han,[b†] Tae Woong Cho,[a] Gyung Hyun Kim,[a] Young Joon Yoo,[a] JuSang Park,[a] Young Jun Kim,[a] Eun Jung Lee,[a] Sihyn Lee,[c] Sungwook Mhin,[c] Sang Yoon Park,[a*] Jeeyoung Yoo[b**] and Sang-hwa Lee[a***]

[a].Advanced Institute of Convergence Technology, Seoul National University, Suwon 16229, Republic of Korea.

[b].School of Energy Engineering, Kyungpook National University, Daegu, 41566, Republic of Korea.

[c].Advanced Materials Engineering, Kyonggi University, Suwon 16227, Republic of Korea.

† These authors equally contributed to this work.

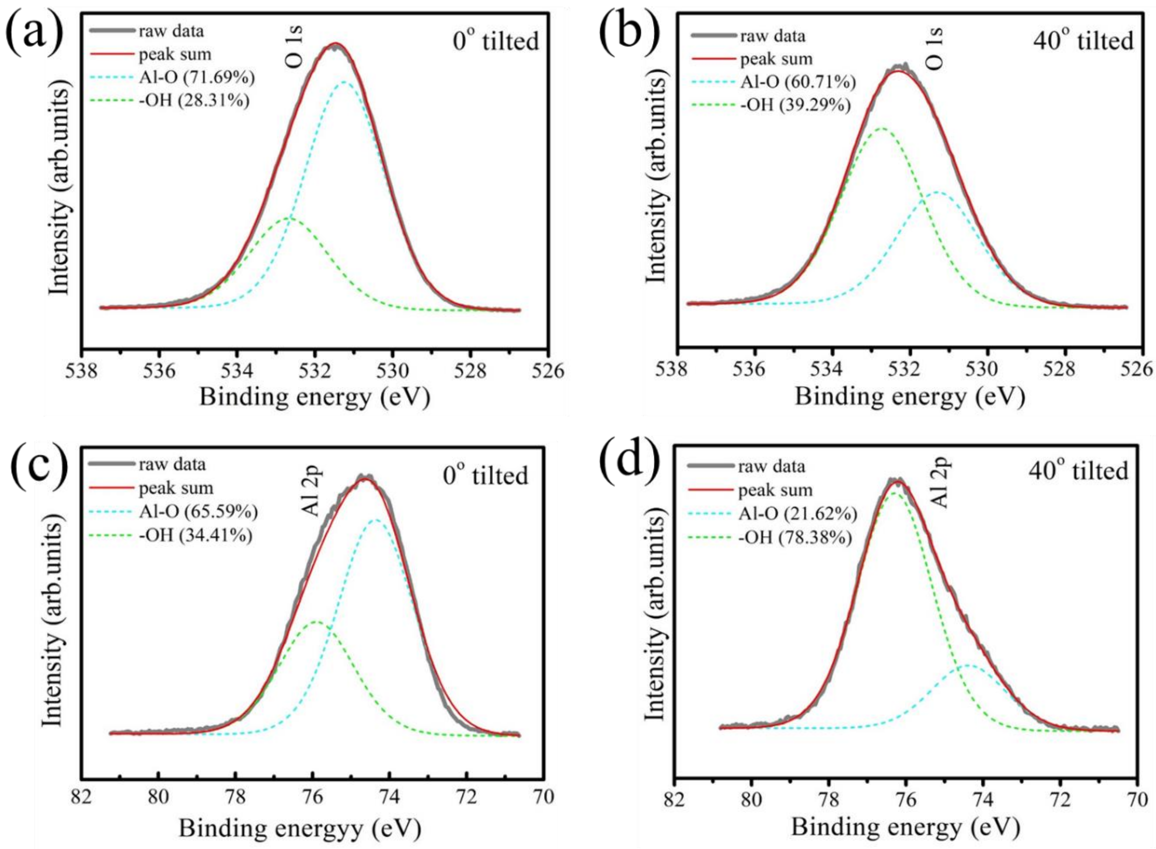

Figure S1. The narrow scan data of XPS spectra for the Al_2O_3@Zn. The normal XPS data for Al 2p and O 1s are shown in (a) and (b), respectively. Angle resolved XPS (ARXPS) data is shown in (c) and (d).

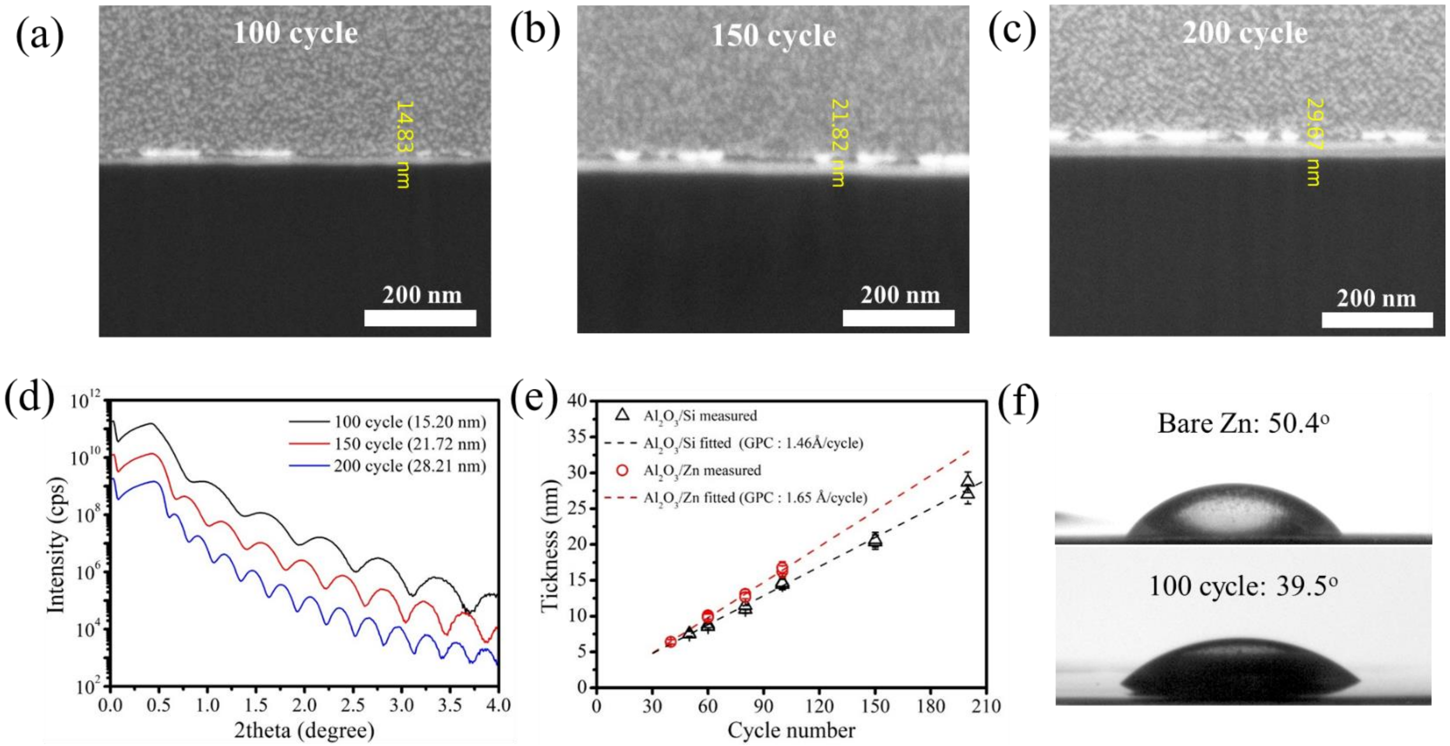

Figure S2. A thickness of the Al_2O_3@Si was analysed by SEM and XRR for the correction of complex refractive index values, which is compatible for the deposited Al_2O_3. The cross-section images of 100, 150, and 200Al_2O_3@Si are shown in (a), (b), and (c), measured by SEM. (d) XRR data of the Al_2O_3@Si (e) The growth rate of the Al_2O_3@Si and Al_2O_3@Zn indicated by growth per cycle (GPC). (f) The contact angles of electrolyte on bare Zn and 100Al_2O_3@Z

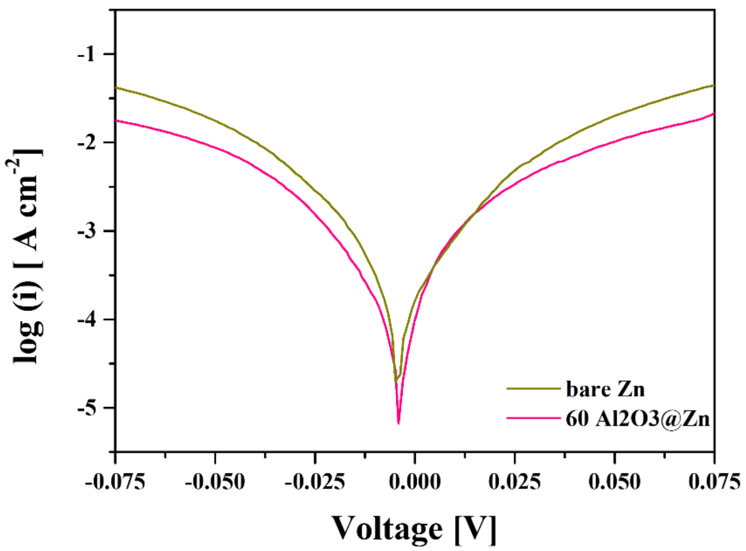

Figure S3. Tafel plot of bare Zn and 60 Al_2O_3@Zn. Linear sweep voltammetry (LSV) was conducted to calculate the corrosion current of the Zn/Zn symmetric cell. The voltage was swept from −150 to 150 mV at a scan rate of 1 mV s^{-1}.

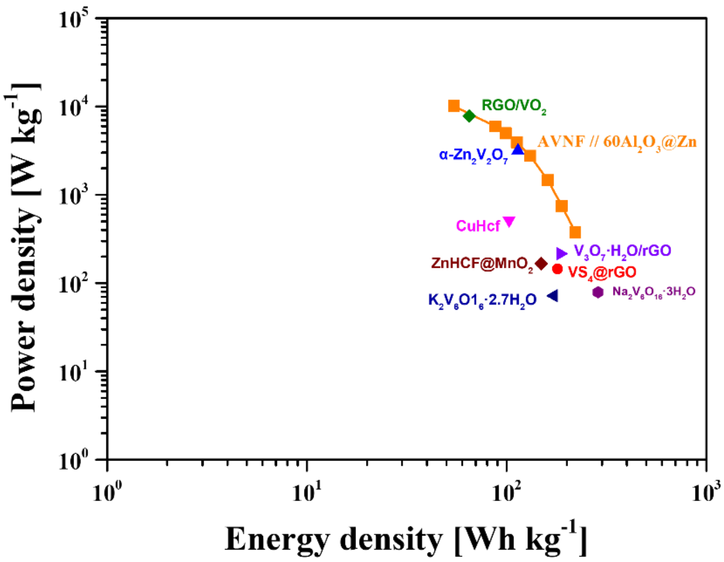

Figure S4. The ragone plot of AVNF//60Al_2O_3@Zn in comparison with other aqueous ZIBs.[59-66]

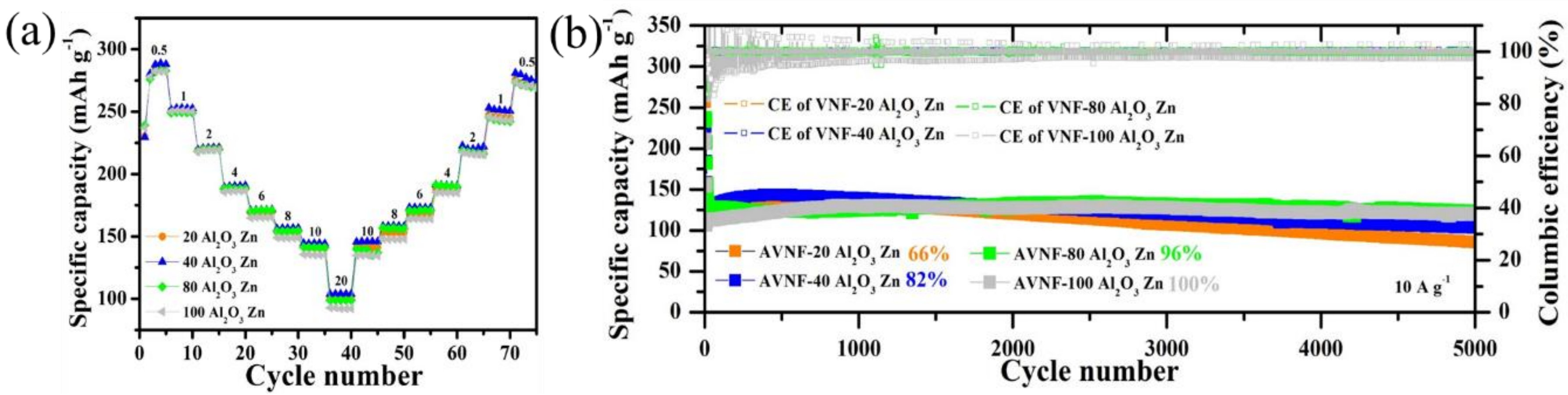

Figure S5. (a) A comparison of rate capabilities and (b) cycling performance of AVNF//Al_2O_3@Zn depending on the ALD cycle, which varied to 20, 40, 80, 100.

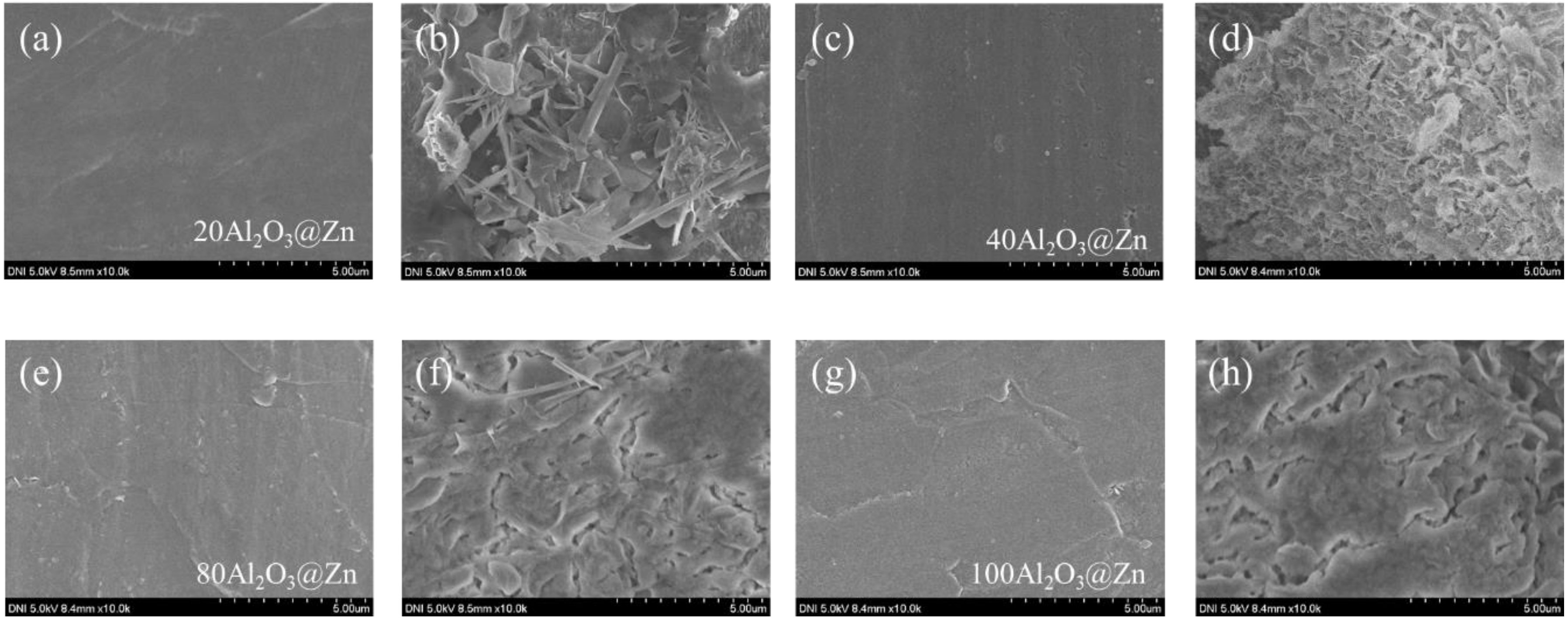

Figure S6. A series of the SEM images (top view) for 20, 40, 80 and $100Al_2O_3$@Zn depending on the electrochemical cycling.

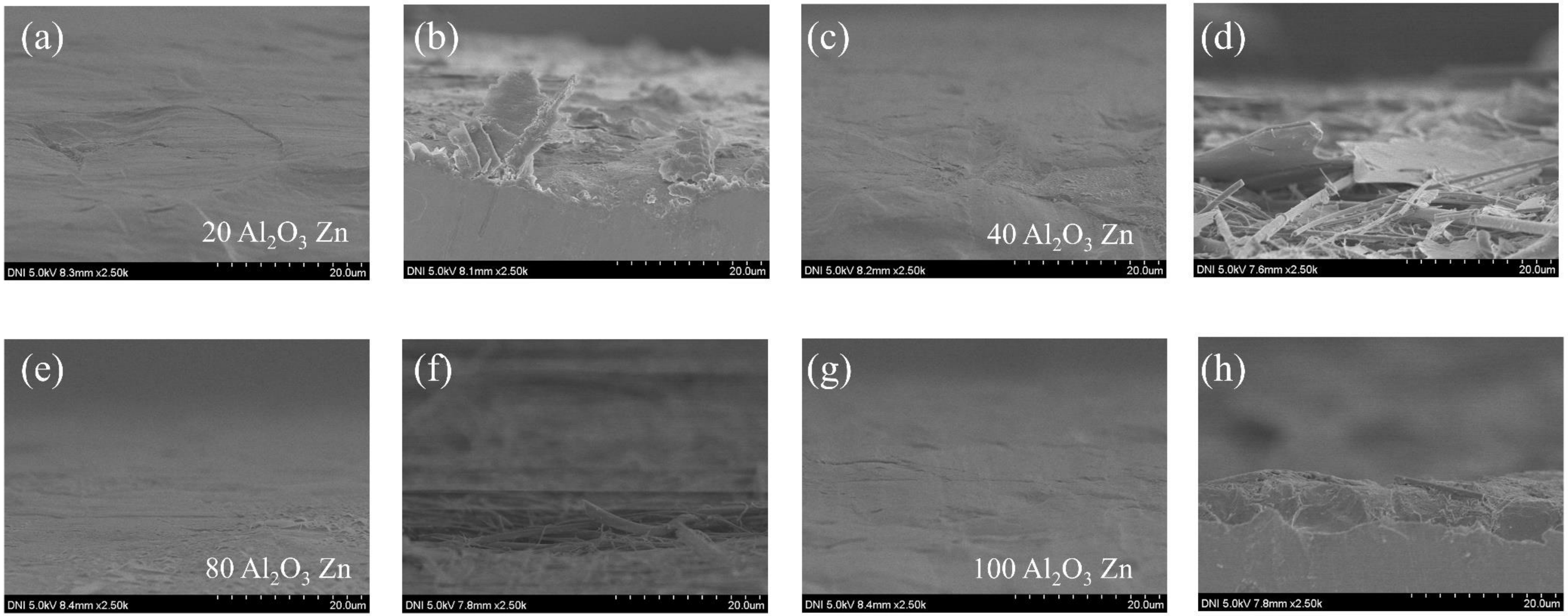

Figure S7. A series of the SEM images (cross-sectional view) for 20, 40, 80 and 100Al_2O_3@Zn depending on the electrochemical cycling.

Reference

59 B. Sambandam, V. Soundharrajan, S. Kim, M. H. Alfaruqi, J. Jo, S. Kim, V. Mathew, Y. K. Sun and J. Kim, Journal of Materials Chemistry A, 2018, **6**, 3850.

60 H. Qin, Z. Yang, L. Chen, X. Chen and L. Wang, Journal of Materials Chemistry A, 2018, **6**, 23757.

61 V. Soundharrajan, B. Sambandam, S. Kim, M. H. Alfaruqi, D. Y. Putro, J. Jo, S. Kim, V. Mathew, Y. K. Sun and J. Kim, Nano Letters, 2018, **18**, 2402.

62 C. Shen, X. Li, N. Li, K. Xie, J. G. Wang, X. Liu and B. Wei, ACS Applied Materials & Inerfaces, 2018, **10**, 25446.

63 X. Dai, F. Wan, L. Zhang, H. Cao and Z. Niu, Energy Storage Materials, 2019, **17**, 143.

64 B. Sambandam, V. Soundharrajan, S. Kim, M. H. Alfaruqi, J. Jo, S. Kim, V. Mathew, Y. K. Sun and J. Kim, Journal of Materials Chemistry A, 2018, **6**, 15530.

65 K. Lu, B. Song, Y. Zhang, H. Ma and J. Zhang, , Journal of Materials Chemistry A, 2017, **5**, 23628.

66 T. Gupta, A. Kim, S. Phadke, S. Biswas, T. Luong, B. J. Hertzberg, M. Chamoun, K. Evans-Lutterodt and D. A. Steingart, Journal of Power Sources, 2016, **305**, 22.